NUMERICAL SIMULATIONS OF COLLAPSE OF FRAMED STRUCTURES

by

Yutaka Toi(I), Hong-Jong Yang(II) and Kazuhiko Obata(III)

1. INTRODUCTION

The purpose of the present study is to develop the economical finite element analysis program for the collapse simulation of framed structures and to verify the validity of the developed code through the comparisons of the numerical results with the test results. In the next section 2, the outline of the developed code is described, in which the linear Timoshenko beam element is employed with the variable location technique of the numerical integration point and the elasto-plastic constitutive equation expressed in terms of resultant forces. In the following sections 3 and 4, the finite element results by the updated Lagrangian formulation are compared with the crush test results conducted for beams, columns and space frames. The strain hardening and the frictional contact are taken into account in the present analysis.

2. OUTLINES OF THE DEVELOPED FINITE ELEMENT CODE [1-3]

The outlines of the developed finite element code for the crush analysis of framed structures are as follows: (1) The linear Timoshenko beam element based on the reduced integration technique (one-point integration) is extended to the three-dimentional finite deformation problem. (2) The location of the occurrence of a plastic hinge in the element is controlled by the movement of the numerical integration point. (3) As for the incremental theory, the total Lagrangian formulation is used for the ultimate strength analysis, while the updated Lagrangian formulation is employed for the crush analysis accompanied by large strains and rotations. (4) The elasto-plastic constitutive equation is expressed in terms of the generalized stresses (i.e. sectional forces) and the generalized strains (such as curvatures) with the strain hardening effect. (5) As for the contact between the loading slab and the test specimen, the penalty function method and the direct control of the nodal displacements are appropriately employed.

The assumed yield function is expressed as

$$f^2 = (M_x/Z_{xp})^2 + (M_y/Z_{yp})^2 + a|N/A|\{(M_x/Z_{xp})^2 + (M_y/Z_{yp})^2\}^{1/2} + (N/A)^2 + 3(M_z/W_p)^2 \quad (1)$$

where N, M_x, M_y and M_z are the axial force, the bending moment about

(I) Associate Professor, Institute of Industrial Science, University of Tokyo (II) Graduate Student, University of Tokyo (III) Assistant, Institute of Industrial Science, University of Tokyo

x-axis, the bending moment about y-axis and the torsional moment, respectively. A is the cross-sectional area. Z_{xp} and Z_{yp} are plastic sectional coefficients, and W_p is the corresponding coefficient for torsion which is given by the following equation for a circular pipe:

$$W_p = \pi(D_o^2 - D_i^2)/12 \tag{2}$$

where D_o and D_i are the outer radius and the inner radius, respectively. The 'a' in eq. (1) is the parameter which determines the shape of the yield surface. It is assumed 0.5 in the present analysis.

3. NONLINEAR COLLAPSE OF BEAMS AND COLUMNS[3]

3.1 Clamped Beam Under Centrally Concentrated Loading

Fig. 1 shows the comparisons between the numerical results and the experimental results for a beam subjected to a centrally concentrated loading, whose ends are both clamped and horizontally free. In the finite element analysis, a half span of the beam was subdivided with five uniform elements. In the loaded and the clamped elements, the numerical integration point is placed at the element edge opposite to the loaded or the clamped end in order to make the plastic hinges form exactly at the loaded or the clamped end. The agreement between the analysis and the experiment is fairly good.

3.2 Fixed Beam Under Centrally Concentrated Loading

Fig. 2 shows the results for a fixed beam subjected to a centrally concentrated loading, whose ends are free from sliding. The assumed mesh is the same as that for the clamped beam in the preceding subsection. A slight difference between the calculated and the experimental load-displacement curves is due to the occurence of the local flattening at the loaded section, as observed in the experimental photo shown in Fig. 2(b).

3.3 Simply Supported Column Under Eccentrically Compressive Loading

The numerical and the experimental results for an eccentrically compressed column with simply supported ends are shown in Fig. 3. A half span was subdivided with ten uniform elements in the finite element analysis. The calculated deformation of the column is in fairly good agreement because of the consideration of a strain-hardening effect.

4. CRUSHING COLLAPSE OF SPACE FRAMES[3]

The crush tests of space frames have been conducted for three loading cases as shown in Fig. 4. The members are connected with each other by the rigid ball, which causes the difficulty of the treatment of frictional contact between the loading slab and the test specimen in the finite element analysis.

4.1 Crush of a Space Frame Under 4-point Loading

Fig. 5 shows the numerical and the expermental results for the space frame under 4-point loading. Four beam members are respectively

subdivided with 20 uniform elements and each one of four columns is subdivided with 40 uniform elements. The difference between the calculated and the experimental load-displacement curves is due to the slight difference of the timing for the buckling of four columns. Both deformations agree well with each other.

4.2 Crush of a Space Frame Under 2-point Loading

Fig. 6 shows the results for the space frame under 2-point loading. The beams and the columns are subdivided with 20 and 30 uniform elements, respectively. The agreement between the numerical and the experimental results is good as a whole.

4.3 Crush of a Space Frame Under 1-point Loading

The calculated results for the space frame under 1-point loading are compared with the experimental results in Fig. 7. Two different frictional coefficients are assumed in the analysis. In the analysis 1, the initial value is 0.2 and later it becomes 0.12, while in the analysis 2, the initial value is 0.2 and later it becomes 0.10. The analysis 1 agrees a little better with the experiment. The present analyses have been conducted with 204 elements, 204 nodes and 546 loading steps. The computing time for each case was 135 seconds in the main frame HITAC M-682H and 965 seconds in the graphic-supercomputer STELLAR GS-1000.

5. CONCLUDING REMARKS

The finite element program for the collapse analysis of three-dimensional framed structures under static loading has been developed and the validity of the developed code has been checked through the comparisons of the numerical results with the test results. The conclusions can be summarized as follows:

(1) From the results for beams and columns, it can be seen that the present analysis method gives sufficiently accurate solutions for the collapse problem accompanied by large strains and large displacements, except for the cases when local deformations as shells are obvious.

(2) From the results for space frames, it can be seen that the developed code is sufficiently economical and accurate from a practical point of view in the crush analysis of three-dimensional framed structures.

REFERENCES

[1] Y. Toi: Nonlinear Dynamic Analysis of Frames and Axisymmetric Shells, J. of the Soc. of Naval Architects of Japan, Vol. 147, (1980), 329.

[2] Y. Toi and H-J Yang: Simulation of Collapse of Framed Structures (Part 1. Formulations and Simple Numerical Examples), J. of the Soc. of Naval Architects of Japan, Vol. 166, (1989), 285.

[3] Y. Toi and H-J Yang: Simulation of Collapse of Framed Structures (Part 2. Comparisons of the Numerical Results with the Experimental Results for the Crush Problem), J. of the Soc. of Naval Architects of Japan, Vol. 167, (1990) to be published.

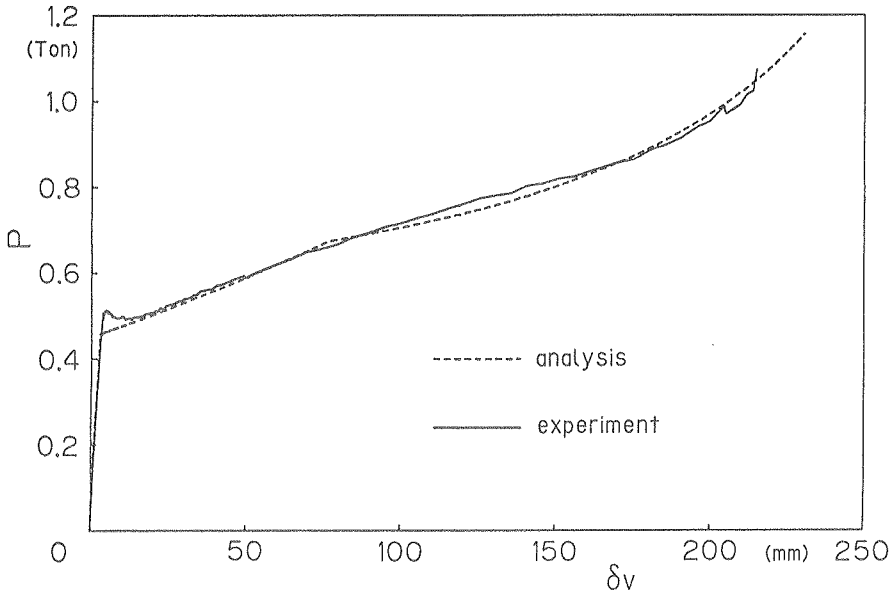

(a) load-deflection curves

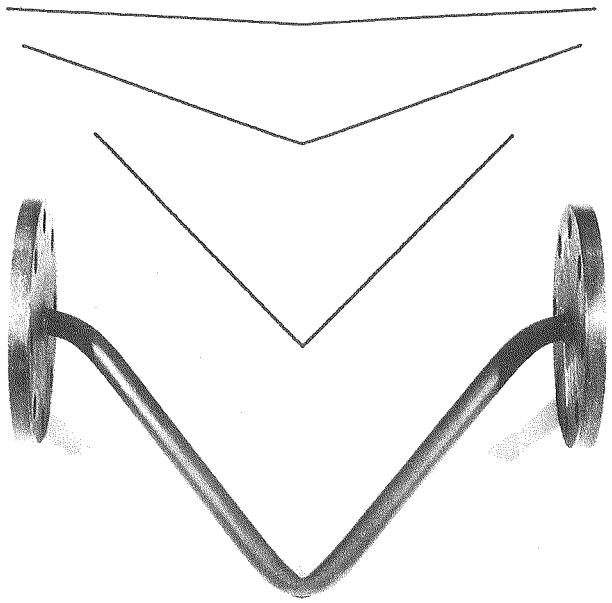

(b) deformed configurations

Fig. 1 Clamped beam under centrally concentrated loading

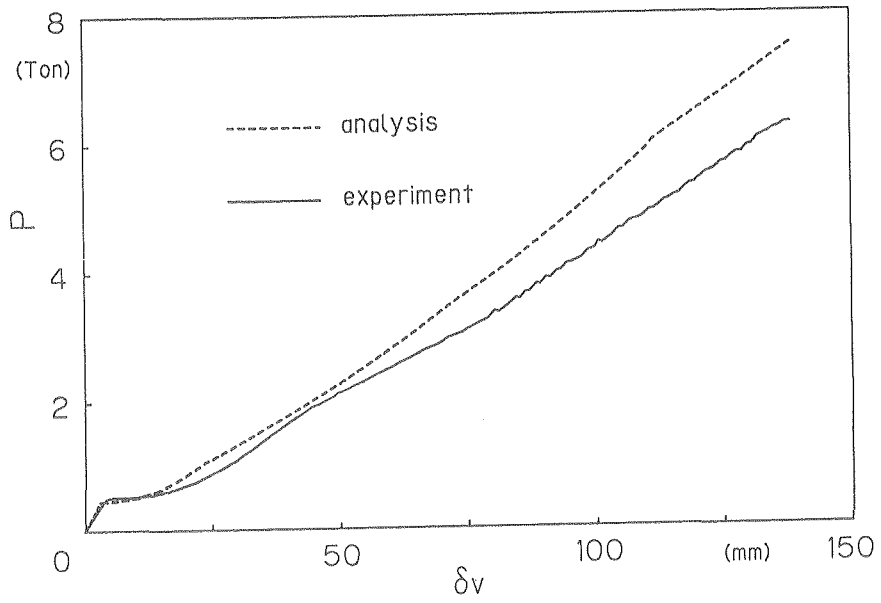

(a) load-deflection curves

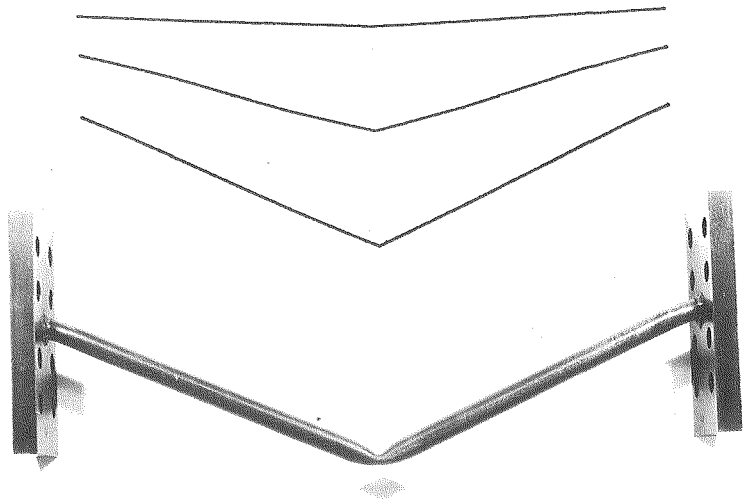

(b) deformed configurations

Fig. 2 Fixed beam under centrally concentrated loading

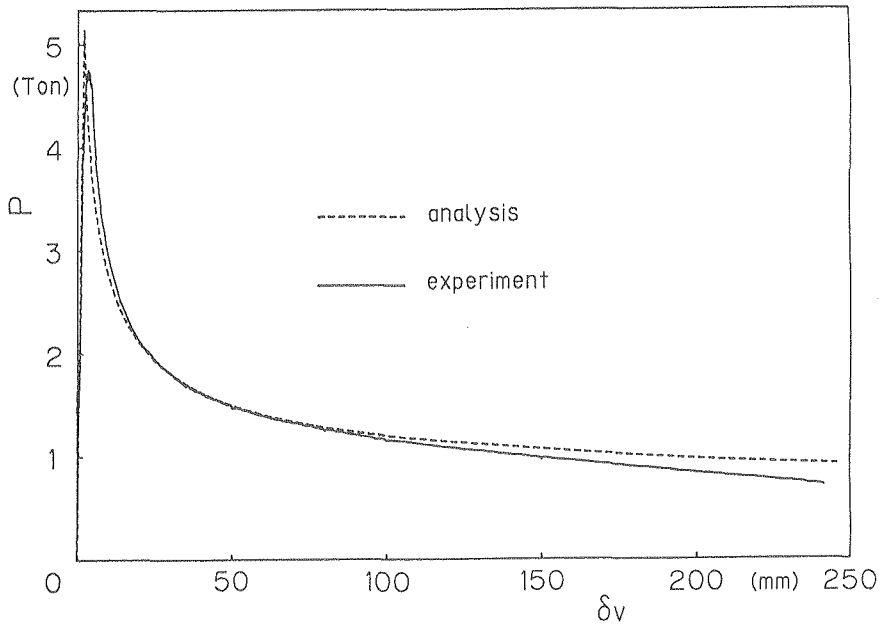

(a) load-shortening curves

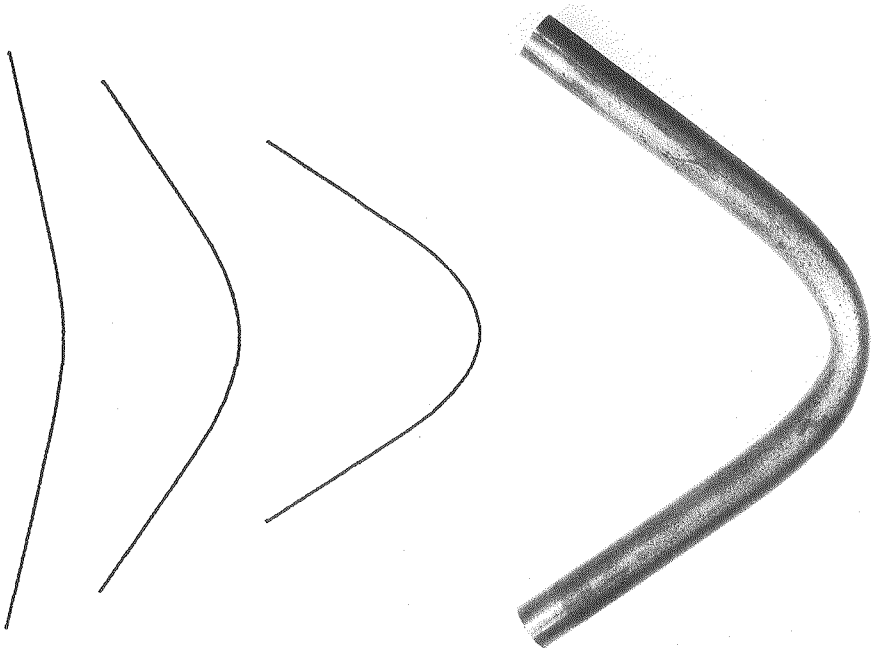

(b) deformed configurations

Fig. 3 Simply supported column under eccentrically compressive loading

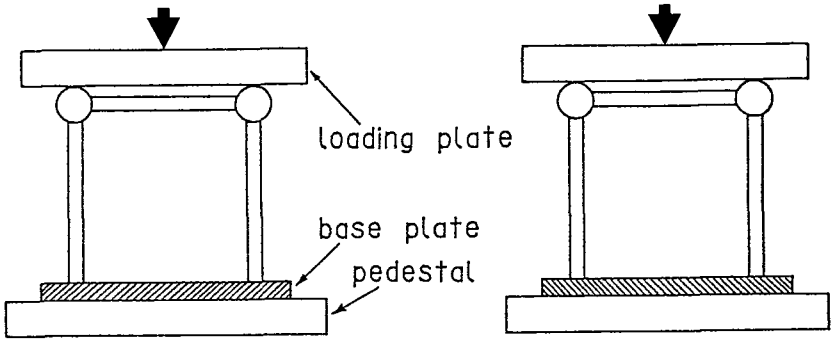

(a) 4-point loading

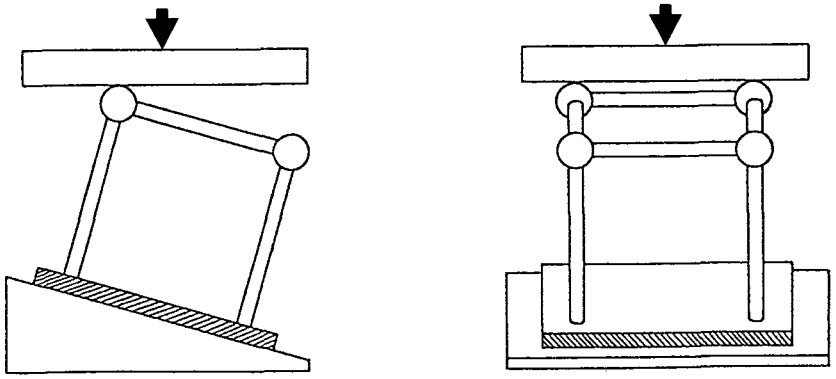

(b) 2-point loading

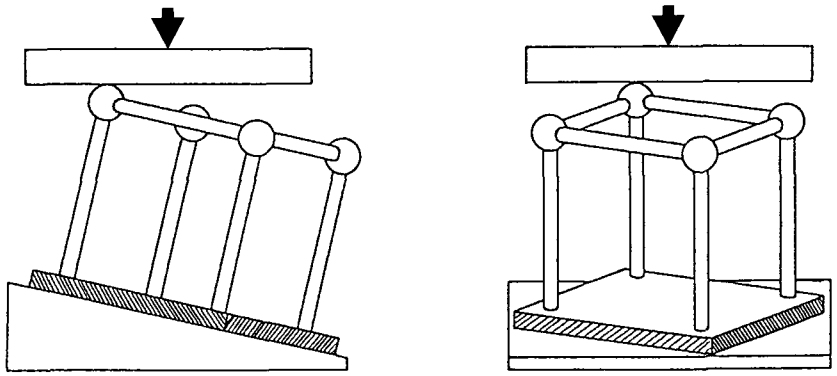

(c) 1-point loading

Fig. 4 Type of loading for a space frame

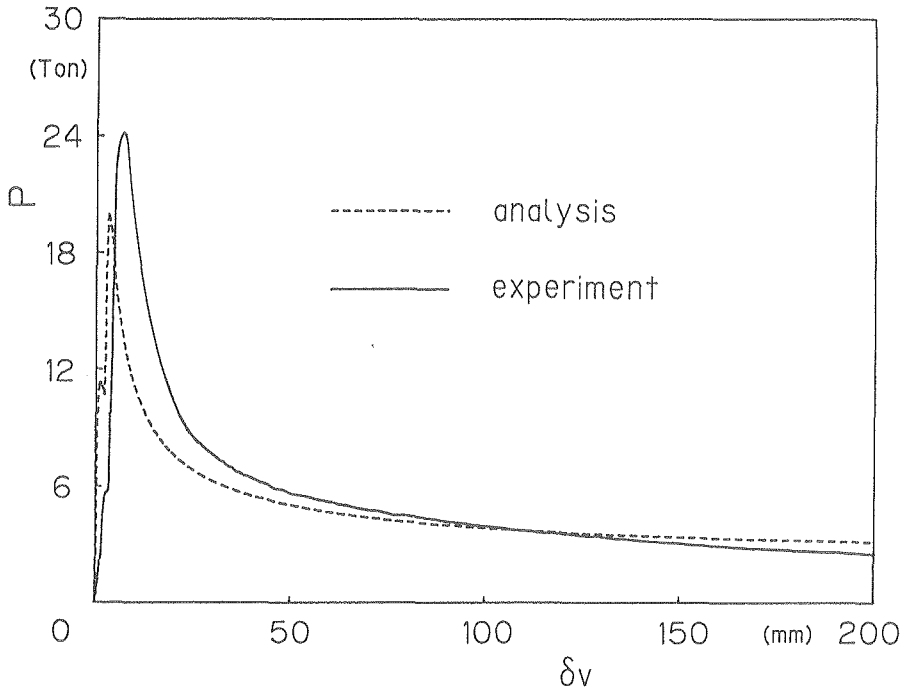

(a) load-displacement curves

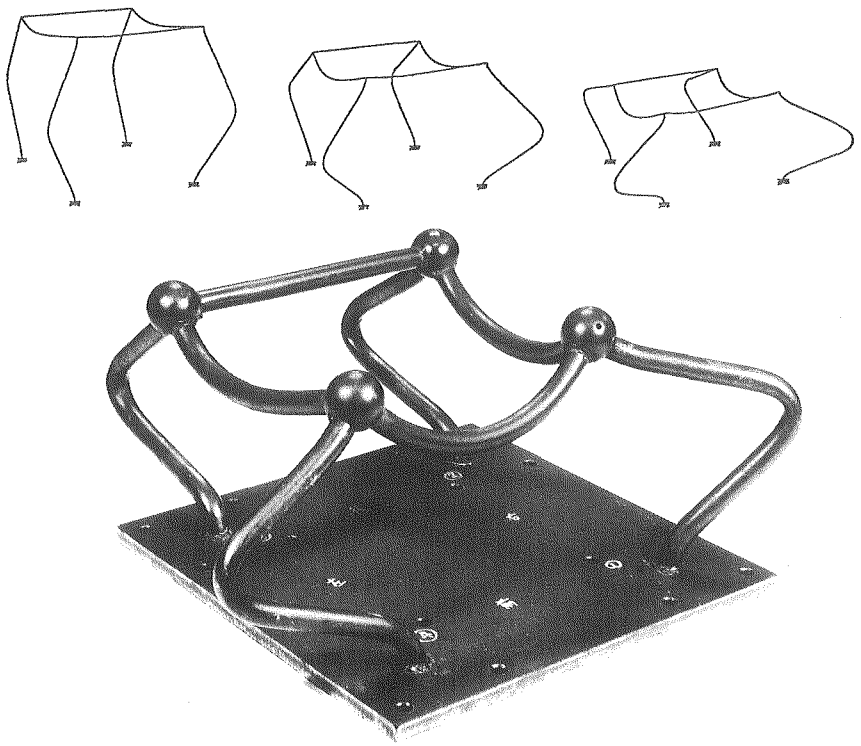

(b) deformed configurations

Fig. 5 Space frame under 4-point loading

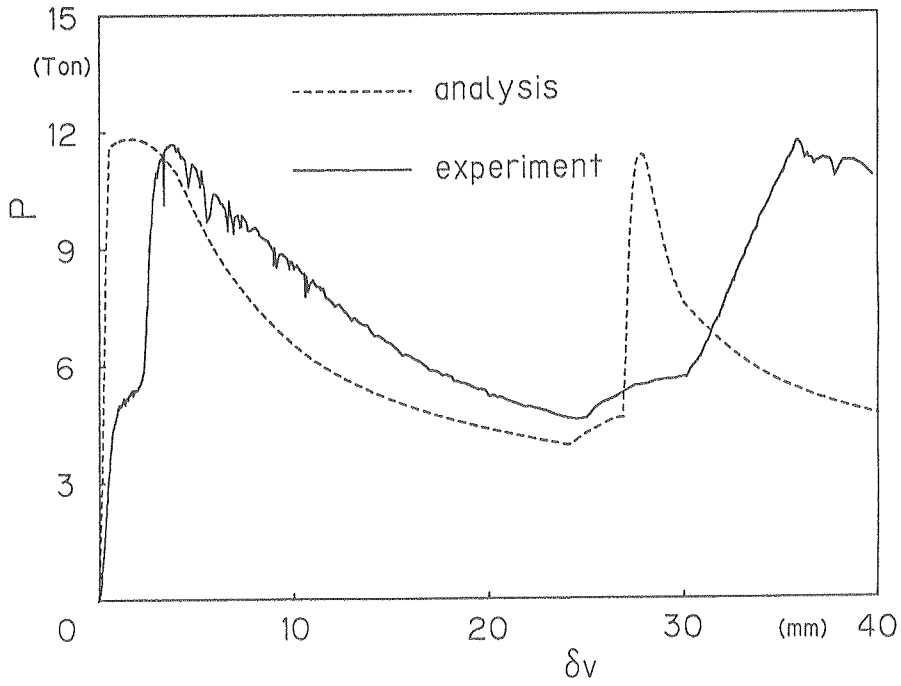

(a) load-displacement curves

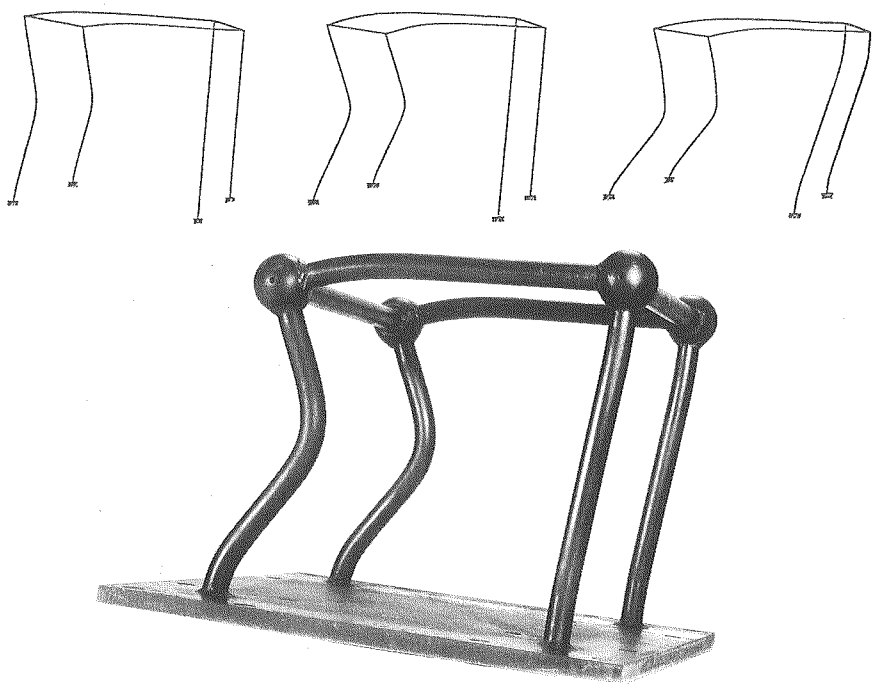

(b) deformed configurations

Fig. 6 Space frame under 2-point loading

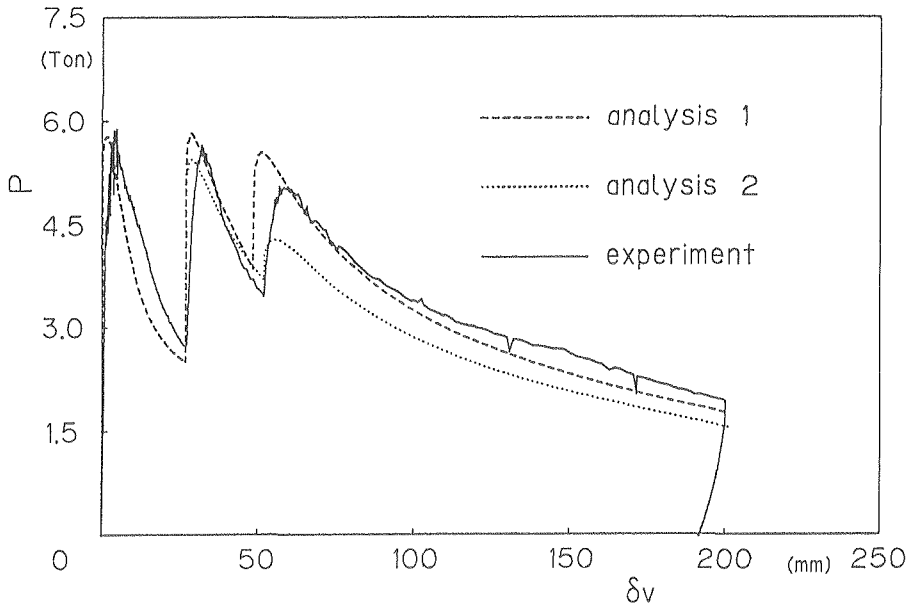

(a) load-displacement curves

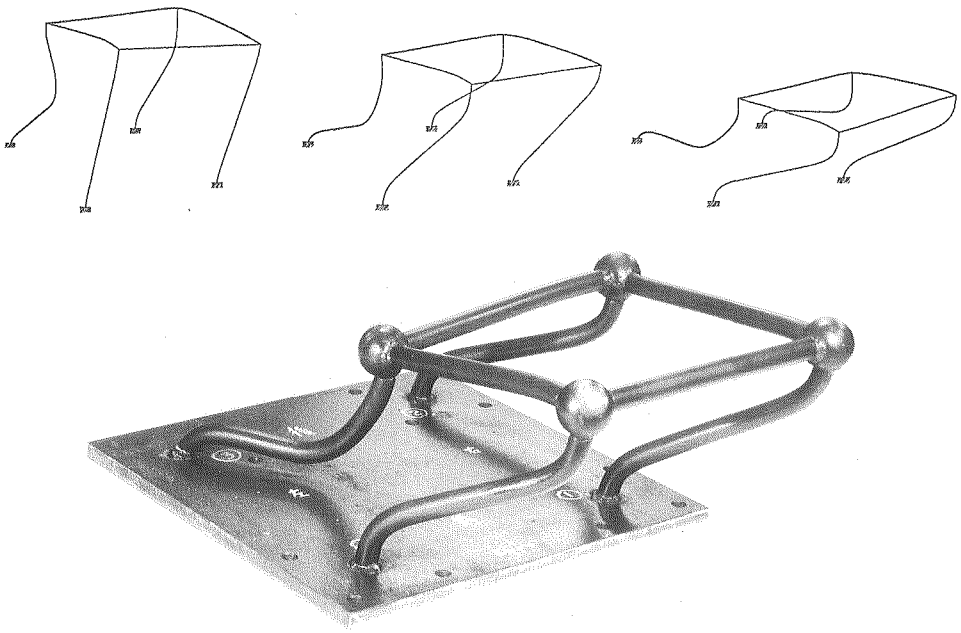

(b) deformed configurations

Fig. 7 Space frame under 1-point loading